Theoretical Investigation of the Chemisorption of H_2 and CO on the ZnO(10$\bar{1}$0) Surface

Maurizio Casarin,*,† Chiara Maccato,† and Andrea Vittadini‡

Dipartimento di Chimica Inorganica, Metallorganica ed Analitica, Università di Padova, Via Loredan 4, Padova, Italy, and Centro di Studio sulla Stabilità e Reattività dei Composti di Coordinazione del CNR, Via Marzolo 1, Padova, Italy

Received April 20, 1998

Density functional molecular cluster calculations have been used to study the adsorption of CO and H_2 on the ZnO(10$\bar{1}$0) surface. Substrate and adsorbate geometry modifications, adsorption energies and adsorbate vibrations are computed in good agreement with experiment. For CO, the influence of Cu surface impurities has been also considered. Despite the limited size of the adopted clusters, surface relaxations computed for the clean and undoped ZnO(10$\bar{1}$0) agree well with experimental measurements. The chemisorption of CO on ZnO(10$\bar{1}$0) relieves some of the relaxation of the Lewis acid site (L_s^a); nevertheless, the L_s^a electronic structure is negligibly affected by the interaction with CO. At variance to that, the stronger interaction of CO with copper impurities significantly influences both the geometry and the electronic structure of L_s^a, extending its effects to the adjacent Lewis base site (L_s^b). The dissociative adsorption of H_2 is found to be exothermic by 23 kcal/mol, and it implies the $L_s^a-L_s^b$ bond breaking.

1. Introduction

Zinc oxide (ZnO) is a wurtzite structured material with appealing properties and applications in electronics,[1] catalysis (e.g., olefin hydrogenation,[2] hydrogenation of CO to give methanol,[3] and oxidation of methane to formaldehyde[4]), and gas-sensor technology. For these reasons, ZnO is probably the most extensively studied non-transition-metal oxide with particular reference to its chemisorption properties.[5] In this regard, it deserves to be emphasized that an intimate comprehension of chemisorption processes on metal oxide surfaces is important because exposed cations on surfaces of these materials have been found to provide the strongest connection between heterogeneous and homogeneous catalysis.[6]

Two forms of H_2 adsorption on ZnO are known: type I, rapid and reversible at room temperature (RT) with a surface coverage ranging from 5 to 10%, and type II, irreversible at RT.[2] It is unanimously accepted that the former type of chemisorption consists of hydrogen heterolytically adsorbed on surface dimers formed by $Zn^{2+}O^{2-}$ pairs to give O−H and Zn−H surface species[7] while the latter seems to be mainly due to an IR inactive species formed by a reductive mechanism contemporary releasing electrons to the ZnO conduction band.[9]

Most experiments concerning the chemisorption of H_2 on ZnO have been carried out on powder samples. The wurtzite structure of ZnO provides a quite large number of low-index surface planes;[10] nevertheless, Scarano et al.[11] have shown that in powders, neutral prismatic (10$\bar{1}$0) and (11$\bar{2}$0) faces are predominant and account for ∼80% of the total surface. As a matter of fact, theoretical investigations so far devoted to type I adsorption of H_2 on ZnO have always modeled the final state of this reaction by considering the heterolytic dissociation of H_2 on the ZnO(10$\bar{1}$0) surface.[12−15] All of these studies were based on the molecular cluster approach, though adopting theoretical schemes of different degrees of sophistication and clusters of different sizes and different embedding techniques. Substrate relaxation was always neglected.

As a part of a research program devoted to the investigation of the ZnO surface reactivity, in the near past we theoretically explored the molecular and dissociative chemisorption of simple Brønsted acids (H_2Y, Y = O and S) on ZnO(10$\bar{1}$0) by coupling the molecular cluster approach to the density functional theory (DFT).[16,17] We found that (i) molecular chemisorption has only

* To whom correspondence should be addressed. Phone: 39-49-8275164. Fax: 39-49-8275161. E-mail: casarin@chim01.unipd.it.

† Università di Padova.

‡ CNR di Padova.

(1) Neumann, G. In *Current Topics in Materials Science*; Ed.; Kaldis, E., North-Holland: Amsterdam, 1981; Vol. 7, p 153.
(2) (a) Kokes, R. J. *Acc. Chem. Res.* **1973**, *6*, 226 and references therein. (b) Kokes, R. J.; Dent, A. L.; Chang, C. C.; Dixon, L. T. *J. Am. Chem. Soc.* **1972**, *94*, 4429.
(3) Waddams, A. L. *Chemicals from Petroleum*, 3rd ed.; Wiley: New York, 1973.
(4) Sojka, Z.; Herman, R. G.; Klier, K. *J. Chem. Soc. Chem. Commun.* **1991**, 185.
(5) (a) Henrich, V. E.; Cox, P. A. *The Surface Science of Metal Oxides*; Cambridge University Press: Cambridge, 1996. (b) Henrich, V. E.; Cox, P. A. *Appl. Surf. Sci.* **1993**, *72*, 277 and references therein.
(6) Barteau, M. A. *J. Vac. Sci. Technol. A* **1993**, *11*, 2162.
(7) Hermann et al.[8] suggested that in the catalyzed synthesis of CH_3OH, the ZnO component of the catalyst plays the role of providing sites for the heterolytic dissociation of H_2.
(8) Hermann, R. G.; Klier, K.; Simmons, G. W.; Finn, B. P.; Bulko, J. B. *J. Catal.* **1979**, *56*, 407.
(9) See, for example: Ghiotti, G.; Chiorino, A.; Bocuzzi, F. *Surf. Sci.* **1993**, *287/288*, 228.
(10) Gay, R. R.; Nodine, M. H.; Henrich, V. E.; Zeiger, H. J.; Solomon, E. I. *J. Am. Chem. Soc.* **1980**, *102*, 6752.
(11) Scarano, D.; Spoto, G.; Bordiga, S.; Zecchina, A.; Lamberti, C. *Surf. Sci.* **1992**, *276*, 281.
(12) Anderson, A. B.; Nichols, J. A. *J. Am. Chem. Soc.* **1986**, *108*, 4742.
(13) Nakatsuji, H.; Fukunishi, Y. *Int. J. Quantum Chem.* **1992**, *42*, 1101.
(14) Nyberg, M.; Nygren, M. A.; Pettersson, L. G. M.; Gay, D. H.; Rohl, A. L. *J. Phys. Chem.* **1996**, *100*, 9054.
(15) (a) Martins, J. B. L.; Andrés, J.; Longo, E.; Taft, C. A. *Int. J. Quantum Chem.* **1996**, *57*, 861. (b) Martins, J. B. L.; Taft, C. A.; Longo, E.; Andrés, J. *J. Mol. Struct. (THEOCHEM)* **1997**, *398−399*, 457.
(16) Casarin, M.; Maccato, C.; Vittadini, A. *Trends Inorg. Chem.* **1996**, *4*, 43.
(17) Casarin, M.; Maccato, C.; Vittadini, A. *Surf. Sci.* **1997**, *377−379*, 587.

10.1021/ic980443s CCC: $15.00
Published on Web 09/25/1998

minor effects on the surface geometry and (ii) the dissociative chemisorption gives rise to *strong* L_s^a-YH and L_s^b-H bonds (L_s^a and L_s^b stand for Lewis acid site and base site, respectively) and to the $L_s^a-L_s^b$ bond breaking.[18] We believe that type I adsorption of H_2 on ZnO($10\bar{1}0$), known to originate from hydroxyl and hydride surface species, could have similar consequences on the structure of the substrate. Therefore, calculations including surface relaxation are needed to settle this matter.

We already mentioned that ZnO shows some catalytic activity for the hydrogenation of CO to CH_3OH.[3] Such an activity is strongly enhanced by the addition of small quantities of Cu. Metallic copper, Cu(I) and Cu(II) sites have been proposed to be the active species for the CH_3OH synthesis, and only a few years ago, it was definitely clarified that the active species is a coordinatively unsaturated tetrahedral Cu(I) site created on ZnO surfaces upon annealing in oxygen.[19]

Recently, our group has extensively applied the molecular cluster approach coupled to DFT to investigate the chemisorption of CO on different materials (ZnO(0001),[20a−c] Cu/ZnO-(0001),[16] CuCl(111),[20d] Cu_2O(111),[21a] Ag_2O(111),[21b] and TiO_2-(110)[21c]). Theoretical results, in excellent agreement with available experimental measurements, allowed us to get a deep understanding of structural and electronic modifications undergone by CO chemisorbed on these substrates. On this basis, we decided to use the adsorption of CO as a test of the capability of the employed clusters to adequately describe adsorption on ZnO($10\bar{1}0$).

2. Computational Details

2.1. Basis Sets. All the calculations have been run by using the DMol method,[22] an ab initio total energy numerical method where the local density functional (LDF) Kohn−Sham equations are solved for systems with a finite size, providing energy eigenvalues, eigenvectors, and charge distribution and allowing the analytic evaluation of energy gradients (force calculations). Exact numerical LDF spherical-atom atomic orbitals (NAOs) are used as basis functions. Because of the quality of these orbitals, basis set superposition effects are minimized and a good description of even weak bonds is possible.[22a]

The following NAOs obtained from LDF calculations relative to free atoms/ions have been employed: (a) Zn, the 1s−4s NAOs of the neutral zinc atom and the 3d−4p NAOs of Zn^{2+}; (b) Cu, the 1s−4s NAOs of the neutral copper atom and the 3d−4p NAOs of Cu^{2+}; (c) O, the 1s−2p NAOs of the neutral oxygen atom the 2s−2p NAOs of O^{2+}, and two sets of 3d, 2p, and 1s NAOs generated from two hydrogenic calculations using $Z = 5$ and 7; (d) C, the 1s−2p NAOs of the neutral carbon atom, the 2s−2p NAOs of C^{2+}, and two sets of 3d, 2p, and 1s NAOs generated from two hydrogenic calculations using $Z = 5$ and 7; (e) H, the 1s NAO of the neutral hydrogen atom and two sets of 1s and 2p NAOs generated from two hydrogenic calculations using $Z = 1.3$ and 4. The pseudatom saturator (H* and H**, see below) basis set is constituted by a single 1s NAO. Throughout the calculations the Zn/Cu 1s−2p NAOs and the O/C 1s NAOs have been kept frozen in a fully occupied configuration, allowing their exclusion from the variational space. Detailed information about the numerical integration scheme is reported in ref 22a. Here, it is sufficient to specify that a number less than or equal to 1000 sample points/atom has been used. As far as the l value of the one-center expansion of the coulomb potential about each nucleus is concerned, a value of l one greater than that in the atomic basis has been found to provide sufficient precision.[22a] As a result of the large size of the investigated systems, we adopted the following degree of angular truncation $l = 3$ for Zn and Cu $l = 2$ for O, C, H, H* and H**.

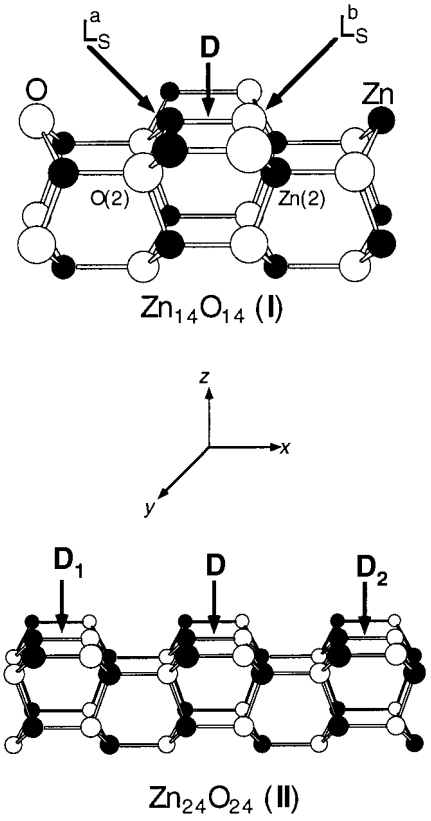

Figure 1. Schematic representation of the clusters (**I** and **II**) adopted to mimic the ZnO($10\bar{1}0$) surface. Pseudoatom saturators are not reported in the figure for the sake of clarity.

2.2. Clusters. Most parts of the numerical experiments have been carried out by modeling the clean and Cu doped ZnO($10\bar{1}0$) surface with the saturated $Zn_{14}O_{14}$ (**I**, see Figure 1) and $CuZn_{13}O_{14}$ (^{Cu}**I**) clusters, respectively.[23] Moreover, a larger saturated cluster ($Zn_{24}O_{24}$−**II**, see Figure 1) has been also used to test the cluster size convergence of the obtained results. Both **I** and **II** have a C_s symmetry and consist of four layers containing the same number of Zn and O ions. The topmost layer is, in both cases, the one representative of the unrelaxed ZnO-($10\bar{1}0$) surface. Within a cluster we distinguish two different kinds of atoms those chemically complete (CCA) and those not chemically complete (NCCA).[24] To avoid the presence of spurious surface states, the NCCAs have been saturated with pseudoatoms to simulate the chaining of the cluster to the rest of the solid. The charge of the pseudoatom saturators has been determined as follows. Each Zn and O CCA participates to four bonds with a total of two and six electrons, respectively. Consequently, all the O NCCAs have been saturated with pseudoatoms H**, each of them carrying a valence charge of 0.5 *e*,

(18) Upon dissociative chemisorption of H_2O (H_2S) on ZnO($10\bar{1}0$), the Zn−O distance passes from 1.845 Å of the relaxed clean surface to 2.28 (2.22) Å; correspondingly, the $L_s^a-L_s^b$ overlap population (OP) decreases from 0.218 *e* to 0.080 *e*.[17]

(19) (a) Didziulis, S. V.; Butcher, K. D.; Cohen, S. L.; Solomon, E. I. *J. Am. Chem. Soc.* **1989**, *111*, 7110. (b) Solomon, E. I.; Jones, P. M.; May, J. *Chem. Rev.* **1993**, *93*, 2623 and references therein.

(20) (a) Casarin, M.; Tondello, E.; Vittadini, A. *Surf. Sci.* **1994**, *303*, 125 and references therein. (b) Casarin, M.; Tondello, E.; Vittadini, A. *Surf. Sci.* **1994**, *307*−*309*, 1182. (c) Casarin, M.; Tondello, E.; Vittadini, A. *Inorg. Chim. Acta* **1995**, *235*, 151. (d) Casarin, M.; Favero, G.; Tondello, E.; Vittadini, A. *Surf. Sci.* **1994**, *317*, 422.

(21) (a) Casarin, M.; Maccato, C.; Vittadini, A. *Surf. Sci.* **1997**, *387*, L1079. (b) Casarin, M.; Maccato, C.; Vittadini, A. *Chem. Phys. Lett.* **1997**, *280*, 53. (c) Casarin, M.; Maccato, C.; Vittadini, A. Submitted for publication.

(22) (a) Delley, B. *J. Chem. Phys.* **1990**, *92*, 508. (b) Delley, B. *J. Chem. Phys.* **1991**, *94*, 7245.

(23) The ZnO backbone of **I** is equivalent to the cluster employed by Anderson and Nichols[12] in their ASED investigation of the dissociative chemisorption of H_2 (type I) on ZnO($10\bar{1}0$).

(24) We consider chemically complete an atom with either a complete shell of nearest neighbors or one, belonging to the topmost layer, missing just one ligand.

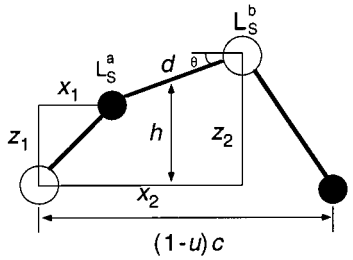

Figure 2. Details of the surface coordinate definitions.

whereas the Zn NCCAs have been saturated with pseudoatoms H*, each of them having a valence charge of 1.5 *e*. A detailed discussion of the reasons which lead us to favor this kind of embedding scheme has been reported elsewhere.[20,21c] The employed O−H** and Zn−H* bond lengths (BLs), 1.088 and 1.625 Å, respectively, have been obtained by minimizing the total energy of tetrahedral pseudomolecules OH_4^{**} and ZnH_4^{*}.

The position of the Zn and O atoms has been determined by using the ideal *c*/*a* ratio (1.633) of the wurtzite hcp lattice rather than the experimental one (1.602).[25] The ideal ratio gives rise to a Zn−O internuclear distance of 1.978 Å to be compared with the experimental ones of 1.992 and 1.973 Å. The experimental mean value of the Zn−O internuclear distance corresponds to the one we have used. Surface relaxation[26] has been partially taken into account by optimizing the *x* and *z* coordinates of the surface dimers (**D** in **I**; **D**, $\mathbf{D_1}$, and $\mathbf{D_2}$ in **II**; see Figure 1).

Vibrational frequencies have been computed through the analytical calculation of the energy gradients and a numerical evaluation of the energy second derivatives within a C_1 symmetry. These calculations have been always carried out by employing clusters **I** and ^{Cu}**I** as representative of the substrate.

Rather than displaying discrete eigenvalues versus an energy axis, we preferred to plot the density of states (DOS) as a function of energy by using a 0.3 eV Lorentzian broadening factor. These plots, based on the Mulliken prescription for partitioning the overlap density,[27] have the advantage of providing insights into the atomic composition of molecular orbitals (MO) over a broad range of energy. The Mulliken population analysis,[27] even though uniquely defined, is rather arbitrary; nevertheless, it is very useful to gain at least a qualitative idea of the electron localization. Selected MO plots have been also reported to assign the character of particular MOs. All the calculations have been performed on a workstation IBM 6000/550 at the inorganic chemistry department of the University of Padova.

3. Results and Discussion

3.1. The Clean and Cu Doped ZnO(10$\bar{1}$0) Surface. The structure of the nonpolar ZnO(10$\bar{1}$0) surface has been debated for a long time.[26] Even though more experimental work is desirable to definitely settle this matter, there is a general consensus about the relaxation of the topmost layer: the oxygen atoms move inward by 0.05 ± 0.1 Å and likewise the Zn ones move inward by 0.45 ± 0.1 Å.[26] Figure 2 shows the coordinates we used to describe the atomic displacements (the same as those adopted in ref 28), while relations between them are reported in Table 1.

As already indicated, the electronic properties of L_s^a and L_s^b on ZnO(10$\bar{1}$0) have been investigated by employing the clusters sketched in Figure 1, limiting the optimization to surface dimers. Optimized geometrical parameters are compared in Table 2 with experimental data[26] as well as with results of other theoretical investigations.[28−30] The inspection of Table 2 points out that the optimized geometry of **D** in **I** and **II** is substantially the same; furthermore, **D**, $\mathbf{D_1}$, and $\mathbf{D_2}$ structures of **II** show negligible differences. These results indicate that even a rather small cluster like **I** is able to capture the main features of the ZnO(10$\bar{1}$0) surface relaxation. In tune with low-energy electron diffraction measurements,[26] L_s^b is displaced inward and likewise L_s^a and the central surface dimer **D** are tilted by an angle of ∼7°; moreover, a significant L_s^a−L_s^b BL shortening is computed (the Zn−O OP of **D** passes from 0.215 to 0.234*e* on moving from the unrelaxed to the relaxed clusters; analogous OP variations are computed for the three surface dimers of **II**). These data agree well with other first-principle studies, the main discrepancy being the prediction of a quite large shift (∼0.15 Å) of the surface dimer center along the *c* axis (i.e., the *x* axis in Figure 1) toward the nearest second-layer zinc atom. It has to be remarked that such a shift has the same absolute value but an opposite direction with respect to that obtained by Schröer et al.[29] through LDA pseudopotentials calculations.[31]

The electronic properties of Cu substitutional impurities on the ZnO(0001) surface have been investigated by Rodriguez and Campbell[32] by means of semiempirical methods applied to bare clusters (they did not provide any embedding scheme). They obtained the following results: (i) the neutral Cu impurity carries substantially the same charge (*Q*) of the Zn ions of the host; (ii) the orbitals strongly localized on the Cu 3d levels are found around the top of the Zn 3d band; (iii) the presence of a substitutional Cu does not significantly modify the position of the highest occupied molecular orbital (HOMO) and the density of states; (vi) *Q*(Cu) of a negatively (−1) charged cluster is ∼1/5 of that of the Zn ions of the host.[33]

Table 1. Coordinate Definitions for the Wurtzite (10$\bar{1}$0) Face and Their Values for the Unrelaxed Surface in Terms of Bulk Lattice Parameters[a]

Coordinate Definitions

$$x_1 = x_{L_s^a}$$
$$x_2 = x_{L_s^b}$$
$$z_1 = z_{L_s^a}$$
$$z_2 = z_{L_s^b}$$

Related Quantities

surface bond length $d = [(x_2 - x_1)^2 + (z_2 - z_1)^2]^{1/2}$

dimer rotation angle $\theta = \arctan\left(\frac{z_2 - z_1}{x_2 - x_1}\right)$

dimer midpoint height $h = \frac{z_2 + z_1}{2}$

dimer midpoint lateral position $x = \frac{x_2 + x_1}{2}$

Unrelaxed Values

$$x_1 = c\left(\frac{1}{2} - u\right) \qquad x_2 = \frac{c}{2}$$
$$z_1 = \frac{a}{2\sqrt{3}} \qquad z_2 = \frac{a}{2\sqrt{3}}$$

[a] From ref 28. Adopted coordinates are displayed in Figure 2.

(25) Abrahams, S. C.; Bernstein, J. L. *Acta Crystallogr. B* **1969**, *25*, 1233.
(26) (a) Duke, C. B. *J. Vac. Sci. Technol. A* **1992**, *10*, 2032. (b) Duke, C. B.; Meyer, R. J.; Paton, A.; Mark, P. *Phys. Rev. B* **1978**, *18*, 4225 and references therein.
(27) Mulliken, R. S. *J. Chem. Phys.* **1955**, *23*, 1833.
(28) Jaffe, J. E.; Harrison, N. M.; Hess, A. C. *Phys. Rev. B* **1994**, *49*, 11153 and references therein.
(29) Schröer, P.; Krüger, P.; Pollmann, J. In *Proceedings of the 4th International Conference on the Formation of Semiconductor Interfaces*; Langeler, B., Luth, H., Mönch W., Pollmann, J., Eds.; World Scientific: Singapore, 1994.
(30) (a) Wang, Y. R.; Duke, C. B. *Surf. Sci.* **1987**, *192*, 307. (b) Wang, Y. R.; Duke, C. B. *Phys. Rev. B* **1987**, *36*, 2763. (c) Wang, Y. R.; Duke, C. B. *Phys. Rev. B* **1987**, *37*, 6417. (d) Wang, Y. R.; Duke, C. B.; Mailhoit, C. *Surf. Sci.* **1987**, *188*, L708.
(31) Tight-binding calculations reported in ref 30 evaluate a 0.291 Å shift of the surface dimer center along the *c* axis towards the nearest second-layer zinc atom.
(32) Rodriguez, J. A.; Campbell, C. T. *J. Phys. Chem.* **1987**, *91*, 6648.

Table 2. Value of Surface Layer Coordinates and Related Quantities for Different Experimental and Theoretical Cases[a]

	x_1 (Å)	x_2 (Å)	z_1 (Å)	z_1 (Å)	$d(L_s^a-L_s^b)$ (Å)	θ (deg)	Δh (Å)	Δx (Å)
bulk exp[b]	0.613	2.605	0.938	0.938	1.992/1.973	0.0	0.0	0.0
surface expt[c]	0.62	2.59	0.54	0.94	2.010	11.5 ± 5	−0.123	−0.004
HF[b]	0.707	2.581	0.691	0.766	1.876	2.31	−0.221	0.034
HF + corr[b]	0.683	2.521	0.678	0.758	1.839	2.48	−0.206	0.035
LDA[d]	0.534	2.365	0.623	0.738	1.835	3.59	−0.258	−0.160
TB[e]	0.98	2.82	0.53	1.10	1.926	17.2	−0.198	0.291
LDA (**I**)[f]	0.856	2.685	0.591	0.827	1.844	7.35	−0.229	0.162
LDA (**II**)[f]	0.863	2.662	0.591	0.845	1.817	8.03	−0.220	0.154
LDA (^{Cu}**I**)[f]	1.123	2.982	0.510	0.943	1.909	13.11	−0.212	0.444

[a] Abbreviations expt and corr stand for experiment and post−SCF correlation calculations. [b] From ref 28. [c] From ref 26. [d] From ref 29. [e] From ref 30. [f] Present work.

Table 3. Selected Effective Mulliken Atomic Charges from Nonrelaxed (NR) and Partially Relaxed (PR) Clusters[a]

	$Zn_{14}O_{14}$ (**I**) (NR)	$Zn_{14}O_{14}$ (**I**) (PR)	$Zn_{24}O_{24}$ (**II**) (NR)	$Zn_{24}O_{24}$ (**II**) (PR)	$CuZn_{13}O_{14}$ (^{Cu}**I**) (PR)
L_s^a	0.84	0.84	0.83	0.81	0.39
L_s^b	−0.86	−0.85	−0.85	−0.83	−0.86
Zn(2)	0.91	0.91	0.89	0.89	0.91
O(2)	−0.90	−0.90	−0.89	−0.89	−0.88

[a] Atom labels as in Figure 1.

We already stressed that most of the numerical experiments concerning Cu substitutional impurities on ZnO($10\bar{1}0$) have been carried out by adopting the saturated $CuZn_{13}O_{14}$ cluster of C_s symmetry. Any attempt to get converged results for the neutral ^{Cu}**I** failed, and the forthcoming discussion about the L_s^a electronic properties of the Cu doped ZnO($10\bar{1}0$) surface refers to data obtained by imposing to ^{Cu}**I** a −1 charge. This is equivalent to assuming a +1 formal oxidation state for the Cu impurity. To verify this point, a further series of calculations has been carried out on the symmetric $CuZn_{21}O_{22}$ cluster, representative of the unrelaxed Cu doped ZnO(0001) surface.[34] Results obtained by using the neutral, bare cluster as well as the saturated, +5 charged one indicate that, at variance to data reported by Rodriguez and Campbell,[32] the Zn/Cu charge ratio is always very close to 2:1.[35] Furthermore, in both cases the HOMOs are localized on the Cu 3d based levels rather than on the O 2p ones, and they lie 5.3 eV lower in energy than the Zn 3d atomlike AOs.

The tendency of the ZnO($10\bar{1}0$) surface cations to change their coordination from a tetrahedral sp^3 to an approximately planar sp^2 hybridization, accompanied by a charge transfer to surface anions that adopt a distorted p^3 configuration,[36] is dramatically enhanced in ^{Cu}**I** (see Table 2), where the L_s^a is only 0.148 Å out of the plane of the oxide ions, which it is bound to. This is not surprising because there are several examples of Cu(I) complexes with a trigonal, planar geometry.[37,38] As far as the L_s^b coordination is concerned, the optimized angle between L_s^a, L_s^b, and the Zn_{nn} ion is 93°.

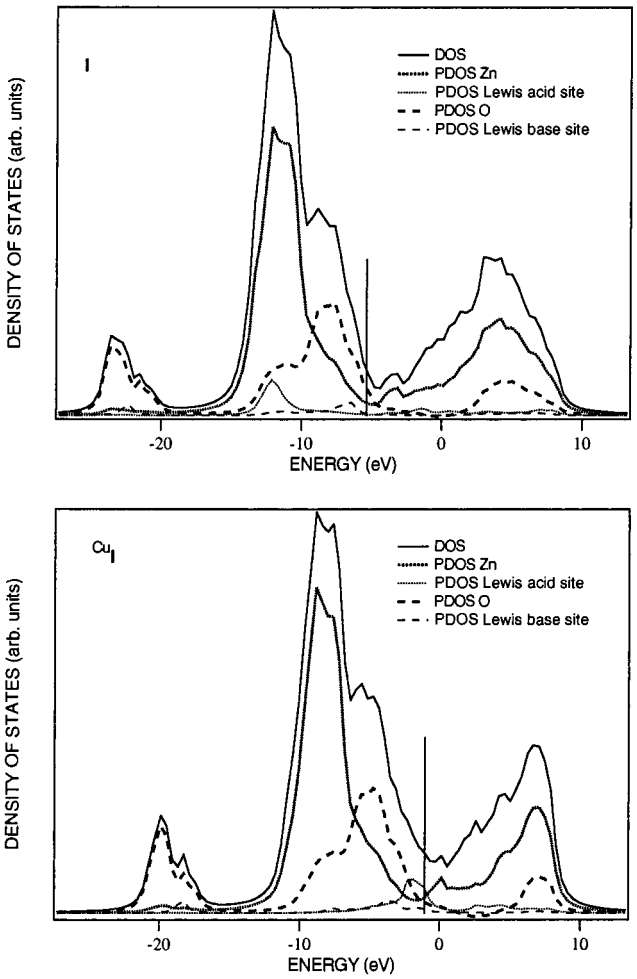

Figure 3. DOS of $Zn_{14}O_{14}H^*_{13}H^{**}_{13}$ and $CuZn_{13}O_{14}H^*_{13}H^{**}_{13}$ clusters. PDOS of L_s^a and L_s^b are also displayed. Vertical bars represent the energy of the highest occupied molecular orbital (HOMO).

In Table 3, the Q values obtained from the Mulliken's population analysis[27] of selected atoms of **I**, **II**, and ^{Cu}**I** are reported. The following considerations can be made: (i) the actual Q values of the ions are significantly smaller than their formal oxidation numbers; (ii) the influence of the partial relaxation on Qs is negligible; (iii) $Q(L_s^a)$ and $Q(L_s^b)$ are smaller than those of CCAs. These results agree well with those we obtained for the unrelaxed, unreconstructed ZnO(0001) polar surface.[20a−c]

In Figure 3, the DOS of clusters **I** and ^{Cu}**I** are reported. As far as cluster **I** is concerned, the agreement with experimental measurements of Gay et al.[10] is good. In detail, three energy

(33) Rodriguez and Campbell[32] pointed out that their negatively charged cluster could be representative of a Cu doped ZnO based catalyst including alkali metals as promoters.

(34) The saturated cluster $L_s^aZn_{21}O_{22}$ has C_{3v} symmetry, and it is the one we used[20a−c] to model the clean and unrelaxed ZnO(0001) surface. It consists of a slab of four layers, each of them constituted by either Zn or O ions. The topmost layer, representative of the polar surface, includes the central L_s^a, six surface nearest neighbors (Zn_{nn}) and three surface next nearest neighbors (Zn_{nnn}). A +5 charge was imposed to the cluster to guarantee that dangling bonds on the Zn surface ions were empty.[20a−c.]

(35) In the bare (saturated, +5 charged) cluster Q(Cu) and $Q(Zn_{nn})$ are 0.39 (0.49) and 0.77 (0.89), respectively.

(36) LaFemina, J. P. *Surf. Sci. Rep.* **1992**, *16*, 133.

(37) Purcell, K. F.; Kotz, J. C. *Inorganic Chemistry*; Hot-Saunders International Editions: Japan, 1985.

(38) Cotton, F. A.; Wilkinson, G. *Advances in Inorganic Chemistry*, 5th ed.; Wiley-Interscience: New York, 1988.

Table 4. Theoretical Results for CO Chemisorbed on the ZnO(10$\bar{1}$0) and Cu/ZnO(10$\bar{1}$0) Surfaces

	I−CO	^{Cu}**I**−CO
$L_s^a-L_s^b$ (Å)	1.853	2.047
L_s^a−CO (Å)	2.055	1.787
C−O (Å)	1.128	1.150
L_s^a−C−O (deg)	161	162
$L_s^b-L_s^a$−C (deg)	95	93
x_1 (Å)	0.796	0.832
x_2 (Å)	2.649	2.868
z_1 (Å)	0.785	1.073
z_2 (Å)	0.790	0.859
ν(C−O) (cm^{-1})	2188	2035
$\nu(L_s^a-C)$ (cm^{-1})	280	494
BE (kcal/mol)	13	28

regions may be identified, (i) the outermost region, extending from about −5.5 to about −8.5 eV and dominated by contributions from the O 2p levels, (ii) the middle region, covering the energy range between about −11 and about −13 eV and mainly due to the corelike Zn 3d AOs, and (iii) the innermost energy region, completely localized on the corelike O 2s levels. Moving to the analysis of the ^{Cu}**I** DOS, besides the overall shift toward higher energies due to the −1 charge of the cluster, we notice that the HOMOs are no more localized on the O 2p levels but instead on the Cu 3d ones. This feature agrees well with valence band photoelectron spectrocopy (PES) data obtained by Didziulis et al.[19a] for the oxidized, low copper coverage (≤0.3 monolayers) ZnO(0001) surface as well as with theoretical outcomes obtained for Cu substitutional impurities on the ZnO-(0001) surface. Incidentally, the energy position of Cu 3d AOs allows us to foresee their possible involvement into the L_s^a−CO interaction.

3.2.1. CO on the ZnO(10$\bar{1}$0) Surface. The interaction between CO and ZnO(10$\bar{1}$0) has been investigated by positioning the CO molecule C-down oriented[39] above the L_s^a of **D** and optimizing the *x* and *z* coordinates of CO and **D**. A further series of numerical experiments with **II**−CO has been carried out to test the cluster-size convergence. Here, the adsorbate has been positioned C-down oriented above the L_s^a of **D** (see Figure 1), extending the optimization to $\mathbf{D_1}$ and $\mathbf{D_2}$. Theoretical results are summarized in Table 4, where data pertaining to **II**−CO are not reported because, on passing from **I**−CO to **II**−CO, negligible geometry variations are computed for **D** and CO. Furthermore, optimized geometrical parameters of $\mathbf{D_1}$ and $\mathbf{D_2}$ are perturbed to a negligible extent upon chemisorption.

The optimized C−O BL is very close to that recently obtained by Jaffe and Hess[40] from ab initio slab calculations (1.122 Å) as well as to our cluster calculations (1.12 Å) for CO on the unrelaxed ZnO(0001).[20a−c] The negligible shortening of the CO BL upon chemisorption (the theoretical C−O BL of the free molecule is 1.129 Å) confirms the picture of a OC−L_s^a bonding limited to a OC → L_s^a σ donation without any L_s^a → CO π back-donation.[41] Looking at Figure 4, where the PDOS of the chemisorbed CO is compared to that of the free molecule, we notice that (i) the CO-based 5σ level undergoes a stabilization energy of ∼2.5 eV upon chemisorption, becoming almost degenerate to the 1π level[42] and (ii) there is no L_s^a → CO back-bonding contribution to the L_s^a−CO interaction. Furthermore, the Q(C) and $Q(O_{CO})$ values (see Table 5) confirm that CO

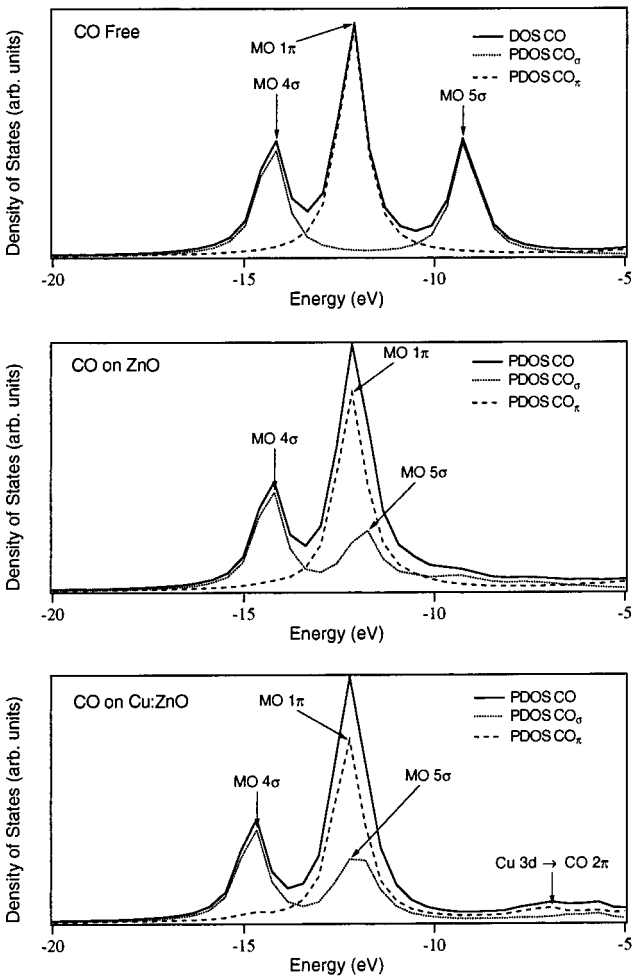

Figure 4. DOS of the free CO molecule (top), PDOS of CO in **I**−CO (middle), and ^{Cu}**I**−CO (bottom). Only occupied states are displayed. In each DOS/PDOS, σ and π contributions are also reported. CO PDOS of **I**−CO and ^{Cu}**I**−CO have been aligned to the inner CO 3σ level, not reported in the figure, to better appreciate variations upon chemisorption.

Table 5. Selected Effective Atomic Charges from Mulliken Population Analysis

	I−CO	^{Cu}**I**−CO
L_s^a	0.82	0.38
L_s^b	−0.85	−0.82
C	0.18	0.17
O	−0.07	−0.20

behaves as a pure donor. Incidentally, the overall charge localized on the adsorbate (+0.11) is very similar to that (+0.13) computed for CO on ZnO(0001).[20a−c] Finally, OPs collected in Table 6 show that in agreement with its weak C−O antibonding nature, the involvement of the CO 5σ HOMO into the OC−L_s^a interaction strengthens the C−O bond (the C−O

(39) It is well-known that on low-index faces of oxides, CO is always adsorbed C-down oriented on surface cations; see, for example: Zecchina, A.; Scarano, D.; Bordiga, S.; Ricchiardi, G.; Spoto, G.; Geobaldo, F. *Catal. Today* **1996**, *27*, 403 and references therein.

(40) Jaffe, J. E.; Hess, A. C. *J. Chem. Phys.* **1996**, *104*, 3348.

(41) In general, the bonding scheme of M−CO carbonyl complexes (M is a transition metal atom in a low oxidation state) is characterized by a two-way electron flow, i.e., a σ donation from the CO 5σ HOMO into M empty levels and a π back-donation from the occupied M *n*d orbitals into the CO 2π lowest unoccupied molecular orbital (LUMO). The absence of any π back-donation from the Zn 3d AOs into the CO LUMO is due to a poor energy matching between the atom like Zn 3d AOs (see Figure 3) and the CO 2π virtual orbitals.

(42) It has been shown that in the case of a *chemical* rather than a *physical* adsorption, the energies of the 1π and 5σ levels are, in contrast to in the gas phase, nearly (within a few tenths of an electronvolt) degenerate in the adsorbate. See: Freund, H. J.; Neumann, M. *Angle-Resolved Photoemission, Theory and Current Application*; Elsevier Science Publishers: Amsterdam, 1992.

Table 6. Selected Overlap Population ($e \times 10^{-3}$) of **I**−CO and ^{Cu}**I**−CO

	I−CO			^{Cu}**I**−CO		
	a′	a″	total	a′	a″	total
L_s^a−L_s^b	174	17	191	123	11	134
L_s^a−C	166	14	180	350	73	423
C−O	404	217	621	388	192	580

OP passes from 0.490*e* in the free molecule[16,20] to 0.621*e* in the chemisorbed one). This outcome finds experimental support in the blue shift undergone by the C−O stretching frequency (ν), which passes from 2143 cm^{-1} in the free molecule[43] to 2202 ± 16 cm^{-1} in the chemisorbed ones.[45]

Literature values of the optimized L_s^a−CO BL range between 1.60 Å,[46] computed by a semiempirical cluster approach, and 2.71 Å, obtained by ab initio periodic calculations.[40] These distances seem to be rather unlikely when compared to BLs (∼1.80−2.10 Å) of terminal carbonyls in organometallic complexes.[37,38] In particular, a L_s^a−CO BL of 1.60 Å with a bonding scheme characterized by the absence of any π back-donation is definitely unrealistic. Furthermore, it can be useful to remember that our optimized value is very close to the ones chosen by Rodriguez and Campbell (2.05 Å)[32] and by Lin et al. (2 Å)[47] for their theoretical investigations.

The optimized L_s^b−L_s^a−C and L_s^a−C−O bond angles (BAs) are 95° and 161°, respectively (see Figure 5). These values do not agree with angle-resolved ultraviolet photoelectron spectra reported by Sayers et al.[48] who found a linear L_s^a−C−O complex and a L_s^b−L_s^a−C BA of ∼120°. Several numerical experiments have been carried out for **I**−CO and **II**−CO with different starting geometries, but all of them converged to the value reported in Table 4.

The coordination of CO to L_s^a has the effect of relieving some of the relaxation of the clean surface (compare the z_1 values in Tables 2 and 4).[49] Nevertheless, the similarity of the L_s^a and L_s^b PDOS of **I** and **I**−CO (see Figure 6) indicates that their electronic structure is only slightly perturbed by the adsorbate. This evidence agrees very well with PES data reported by Didziulis et al.[19a] for CO on ZnO(10$\bar{1}$0) (spectral features of the clean ZnO(10$\bar{1}$0) are unchanged upon chemisorption).

The computed BE of CO to ZnO(10$\bar{1}$0) is in excellent agreement with data reported by Gay et al.[10,50] and Bolis et al.[51] but is significantly lower than that we computed for CO on the unrelaxed ZnO(0001) (27 kcal/mol).[20a−c] One of referees suggested that we investigate the role played by surface relaxation in determining the CO−ZnO(0001) BE. A further series of numerical experiments has been then carried out by modeling the clean ZnO(0001) through the cluster described in ref 34 and optimizing the L_s^a position within the usual constraint of maintaining the symmetry of the cluster (C_{3v}). The results of these calculations can be summarized as follows: (i) the L_s^a of the clean surface relaxes into the 3-fold site described by the coordinated oxide ions by 0.329 Å; (ii) the chemisorption of the CO molecule forces L_s^a to unrelax;[52] (iii) the L_s^a−CO BE is 18 kcal/mol. The L_s^a−CO BE value computed by including

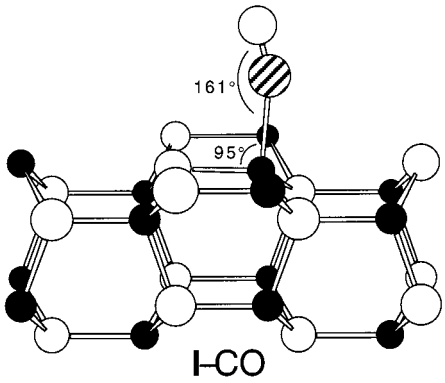

Figure 5. Schematic representation of the optimized geometry of **I**−CO. Pseudoatom saturators are not reported in the figure for the sake of clarity.

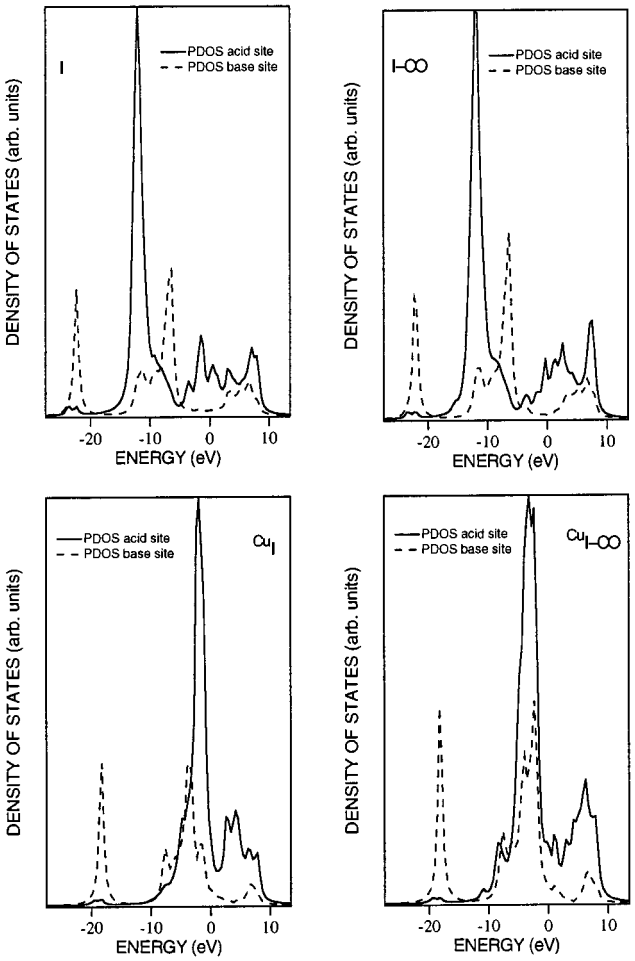

Figure 6. Comparison of the L_s^a and L_s^b PDOS of **I**/**I**−CO and ^{Cu}**I**/^{Cu}**I**−CO.

(43) The experimental stretching frequency of the free CO is 2143 cm^{-1} with a harmonic component of 2170 cm^{-1}.[44] The computed value of the harmonic component of the *free* C−O stretching frequency is 2169 cm^{-1}.

(44) Huber, K. P.; Herzberg, G. *Molecular Spectra and Molecular Structures. Constants of Diatomic Molecules*; Van Nostrand Reinhold Co.: New York, 1979; Vol. 4.

(45) D'Amico, K. L.; McFeely, F. R.; Solomon, E. I. *J. Am. Chem. Soc.* **1983**, *105*, 6380.

(46) Anderson, A. B.; Nichols, J. A. *J. Am. Chem. Soc.* **1986**, *108*, 1385.

(47) Lin, J.; Jones, P.; Guckert, J.; Solomon, E. I. *J. Am. Chem. Soc.* **1991**, *113*, 8312.

(48) Sayers, M. J.; McClellen, M. R.; Gay, R. R.; Solomon, E. I.; McFeely, F. R. *Chem. Phys. Lett.* **1980**, *75*, 575.

(49) Variations of the L_s^a coordinates upon chemisorption are accompanied by a slight increase of the L_s^a−L_s^b BL (1.844 and 1.891 Å in I and I−CO, respectively) which gives rise to a concomitant decrease of the L_s^a−L_s^b OP (see Table 6).

(50) Gay et al.[10] measured the same BE (12 kcal/mol) for CO chemisorbed on polar ((0001) and (000$\bar{1}$)) and non polar ((10$\bar{1}$0) and (11$\bar{2}$0)) ZnO surfaces. Furthermore, the same BE value was obtained by Bolis et al.[51] for CO chemisorbed on ZnO powder samples.

(51) Bolis, V.; Fubini, B.; Giamello, E.; Reller, A. *J. Chem. Soc., Faraday Trans. 1* **1989**, *95*, 855.

the relaxation of L_s^a agrees much better with experiment than that obtained by limiting the optimization to the adsorbate. Nevertheless, it still seems in contrast with the experimental finding of very similar CO−ZnO BEs[10,50] for chemically different ZnO surfaces.[53] In this respect, it is useful to remember that the scanning tunneling microscopy data of Thibado et al.[54] indicate that the ZnO(0001) real surface is actually constituted by terraces of the order of 100 × 100 Å^2 with a large fraction of surface atoms residing on terrace edges. These edges are formed by inclined facets not perpendicular to the surface, having the same characteristic features observed for the O-terminated surface. The morphology of the ZnO(0001) as obtained by such measurements seems to indicate that the chemisorpion on the actual surface is more similar to the chemisorption on powders than on a perfect bulk terminated surface. This could explain why both CO[10] and H_2S[55] have very close adsorption patterns on ZnO(0001) and ZnO(10$\bar{1}$0).

As far as vibrations of CO on ZnO(10$\bar{1}$0) are concerned, FTIR spectroscopy indicates a $\Delta\nu_{C-O}$ of +47 cm^{-1} upon chemisorption on ZnO powders (kadox) in the zero coverage limit.[39] High-resolution electron energy loss spectroscopy results collected on ZnO(10$\bar{1}$0)[45] confirm the ν_{C-O} blue shift with the presence of a band lying at 2202 ± 16 cm^{-1} (the L_s^a−CO stretching is found at 250 ± 16 cm^{-1}). Again, the agreement between experiment and theory is very good (see Table 4).

3.2.2. CO on the Cu-Doped ZnO(10$\bar{1}$0) Surface. The orientation of CO on the Cu-doped substrate is very similar to that found on ZnO(10$\bar{1}$0) (see Table 4). Nevertheless, BL, BE, Q, OP and ν values (see Tables 4−6) indicate that the L_s^a−CO bonding scheme is significantly different on passing from the Zn−CO to the Cu−CO surface complex. In detail, (i) the lengthening of the C−O BL, (ii) the shortening of the L_s^a−C BL, (iii) the small, negative Q_{CO}, (iv) the increasing of the L_s^a−C π OP, (v) the decreasing of the C−O π OP,[56] (vi) the larger adsorbate−substrate BE, and (vii) the dramatic decrease of ν_{C-O} prove that, besides a strong OC → L_s^a σ donation, a concomitant L_s^a → CO π back-donation is present (see Figure 4). In Figure 7, the contour plot of the MO accounting for the L_s^a → CO π interaction in the *xz* plane is displayed.

Once again, the comparison of theoretical outcomes with PES data obtained by Didziulis et al.[19a] for CO chemisorbed on the oxidized, low copper coverage ZnO(0001) and ZnO(10$\bar{1}$0) surfaces is fruitful. Actually, the inspection of Figure 6 clearly indicates that, in agreement with experiment,[19a] a portion of the Cu d band is shifted to lower energy as a consequence of the involvement of suitable d orbitals into the L_s^a → CO π back-bonding. It is noteworthy that the CO adsorption, though occurring molecularly, not only perturbs the electronic structure of **D** but also its geometry (see Tables 2 and 4). As foreseen in section 3.1, the significant participation of the Cu 3d AOs in the L_s^a−CO bonding is simply due to their energy position, higher than that of the atomlike Zn 3d levels.

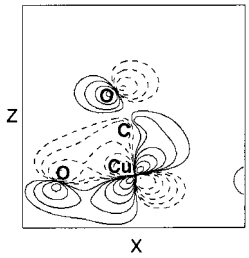

Figure 7. Two-dimensional contour plots of the ^{Cu}**I**−CO 107a′ MO in the *xz* plane. Contour values are ±3.2 × 10^{-3}, ±6.4 × 10^{-3}, ±1.28 × 10^{-2},... $e^{1/2}$/Å$^{3/2}$ with negative values in dashed lines.

Before going on, it deserves to be remarked that the short L_s^a−C and the quite long C−O BLs (1.787 and 1.150 Å, respectively) accompanied by the quite large L_s^a−C π OP (see Table 6)[56] make the Cu−CO bonding scheme very similar to that found in mono- and binuclear Cu(I)−carbonyl complexes.[57] This represents a further confirmation of the Barteau assessment[6] that there is a close analogy between classical coordination chemistry and the surface reactivity of metal centers in oxidized state and metal oxides. Concerning the vibrational parameters of the Cu(I)−CO surface complex, no experimental data are available for comparison.

The Solomon group pointed out in a series of seminal papers[19b,47] that the exposed Cu(I) ions of the polar CuCl(111) surface mimic the electronic structure of unsaturated Cu(I) substitutional impurity in ZnO activated catalysts much better than the exposed Cu(I) cations of Cu_2O(111). We already studied the chemisorption of CO on CuCl(111)[20d] and Cu_2O-(111)[21a−b] so that we have here the opportunity to theoretically test the validity of the Solomon proposal.

In Table 7, selected theoretical results relative to CO on Cu/ZnO(10$\bar{1}$0) are compared with those pertaining to CO on Cu/ZnO(0001),[16] CuCl(111),[20d] and Cu_2O(111).[21a−b] The L_s^a−CO bonding scheme is characterized by a two-way electron flow, and differences in the CO → L_s^a σ donation and L_s^a → CO π back-donation can be analyzed by referring to different *Q* and OP values.[20c] Actually, the stronger the σ donation is, the greater *Q*(C) (the smaller is $Q(L_s^a)$), while the stronger the π back-donation is, the more negative *Q*(O) (the more positive is $Q(L_s^a)$). Furthermore, the stronger the CO → L_s^a interaction is, the greater the L_s^a−C and C−O σ OPs; the stronger the L_s^a → CO back-donation is , the greater (smaller) the L_s^a−C (C−O) π OP.

The analysis of Q and OP values reported in Table 7 points out that at variance to the π L_s^a−CO interaction, the extent of which is quite constant along the series, the σ bonding of CO to Cu_2O(111)[58] is dramatically stronger than that involving the other Cu(I) ions, all of them characterized by a coordination

(52) Upon chemisorption, L_s^a relax into the 3-fold site by −0.062 Å. Optimized L_s^a−C and C−O BLs are 2.201 and 1.121 Å, respectively.

(53) The different L_s^a−CO BE for CO on ZnO(0001) and ZnO(10$\bar{1}$0) has to be ultimately traced back to the stronger electrostatic interaction between the CO dipole moment and Zn^{2+} ions of the polar ZnO(0001) surface.

(54) Thibado, P. M.; Rohrer, G. S.; Bonnell, D. A. *Surf. Sci.* **1994**, *318*, 379.

(55) Lin, J.; May, J. A.; Didziulis, S. V.; Solomon, E. I. *J. Am. Chem. Soc.* **1992**, *114*, 4718.

(56) **I**−CO and ^{Cu}**I**−CO have a C_s symmetry. In the adopted framework, the symmetry plane corresponds to the *xz* one; thus, both *x* and *z* transform as a′, and the pure π character is accounted by the *y* coordinate (a″ in symmetry). This means that the a′ irreducible representation includes both "σ" (*z*) and "π" (*x*) contributions. Nevertheless, a careful inspection of the Mulliken population analysis indicates, for both clusters, a quite poor overlap between π and σ AOs of a′ symmetry, and consequently, a qualitative estimate of σ and π contributions to bonding interactions can be obtained by subtracting the a OP value from the a′ one and doubling the a″ OP value, respectively.

(57) (a) Pasquali, M.; Floriani, C.; Gaetani-Manfredotti, A. *Inorg. Chem.* **1980**, *19*, 1191. (b) Ruggiero, C. E.; Carrier, S. M.; Antholine, W. E.; Whittaker, J. W.; Cramer, C. J.; Tolman, W. B. *J. Am. Chem. Soc.* **1993**, *115*, 11285.

(58) The Cu_2O lattice is highly symmetric. It has a cubic structure where each oxygen is at the centre of a tetrahedron of copper atoms having coordination number two (linearly coordinated to two oxide ions). The unsaturated L_s^a on the clean Cu_2O(111) surface is coordinated to a single oxide ion.

Table 7. Comparison of Selected Theoretical Outcomes for CO Chemisorbed on Cu/ZnO(10$\bar{1}$0), Cu/ZnO(0001), CuCl(111), and Cu_2O(111) Surfaces

		Cu/ZnO(10$\bar{1}$0)	Cu/ZnO(0001)[a]	Cu/ZnO(0001)[b]	CuCl(111)[c]	Cu_2O(111)[d]
L_s^a−C	(Å)	1.79	1.87	1.83	1.84	1.77
C−O	(Å)	1.15	1.13	1.14	1.13	1.14
Q(L_s^a)		0.38	0.41	0.38	0.31	0.17
Q(C)		0.17	0.14	0.11	0.23	0.36
Q(O)		−0.20	−0.05	−0.08	−0.13	−0.13
OP(C−O)	($e \times 10^{-3}$)	580[e] (388 + 192)	620[f] (204 + 416)	612[f] (202 + 410)	661[f] (243 + 418)	702[f] (304 + 398)
OP(L_s^a−C)	($e \times 10^{-3}$)	423[e] (350 + 73)	382[f] (264 + 118)	414[f] (280 + 134)	378[f] (276 + 102)	428[f] (304 + 124)
$E_{4s} - E_{3d}$	(eV)	4.9	4.9	4.9	4.9	2.8
ν(C−O)	(cm^{-1})	2035	2119	2102	2155[g]	2130
ν(L_s^a−C)	(cm^{-1})	494	338	402	415[g]	518
−BE	(kcal/mol)	28	31	33	36	48

[a] Computed by employing the saturated $CuZn_{21}O_{22}$ +5 charged cluster. [b] From ref 16 with the saturated $CuZn_{21}O_{22}$ +4 charged cluster. [c] From ref 20d. [d] From ref 21a. [e] In parentheses, a′ and a″ contributions to the total OP (see note 56). [f] In parentheses, a_1 (σ) and e (π) contributions, respectively, to the total OP. [g] Vibrational frequencies computed through the method reported in section 2, rather than as in ref 20d.

number equal to 3. We have rationalized these results by considering the energy difference between the maxima of the L_s^a 4s and 3d PDOS, also reported in Table 7.[59] If we assume the energy position of the completely occupied Cu 3d AOs as a reference, the ΔE between 4s and 3d AOs along the series indicates that the 4s virtual level of the exposed Cu(I) ions of the Cu_2O(111) surface has the best energy matching with the CO-based 5σ MO. In other words, the unsaturated Cu(I) ions of the Cu_2O(111) surface have the strongest Lewis acidity.

Data reported in Table 7 confirm and reinforce the Solomon proposal[19b,47] that the unsaturated Cu(I) ions of the CuCl(111) polar surface reasonably model the electronic structure of Cu substitutional impurities on ZnO surfaces. However, it has also to be emphasized that our calculations seem to be in contrast with measurements carried out by Didziulis et al.[19a] who evaluated similar BEs for CO bound to unsaturated L_s^a of Cu_2O and to the C_{3v} (unsaturated tetrahedral) Cu(I) ion of the oxidized, low copper coverage ZnO(0001) surface.

3.2.3. Heterolytic Chemisorption of H_2 (Type I) on the ZnO(10$\bar{1}$0) Surface. The heterolytic dissociation of H_2 on the ZnO(10$\bar{1}$0) surface has been studied by positioning the dissociated H_2 molecule above the dimer **D** of **I**, one H atom above L_s^a (H_{Zn}) and the other above L_s^b (H_O), and optimizing the *x* and *z* coordinates of the H atoms and **D**. As in the CO case, a further series of numerical experiments has been carried out by considering cluster **II** as representative of the substrate. Theoretical results pertaining to both series of calculations are collected in Table 8.

In agreement with data obtained for the dissociative chemisorption of H_2O and H_2S on ZnO(10$\bar{1}$0)[17] and with our starting hypothesis, theoretical outcomes for both clusters state that the formation of hydride and hydroxyl surface species is accompanied by the L_s^a−L_s^b bond breaking. Nevertheless, the L_s^a and L_s^b final positions and consequently the H_{Zn} and H_O ones are very different on passing from **I**−H_2 to **II**−H_2. A tentative explanation of such a finding is the presence, in **I**−H_2, of a spurious interaction between L_s^a (L_s^b) and the saturated O (Zn) atom lying in the symmetry plane (see Figure 1), which takes place during the optimization procedure. The forthcoming discussion will be then based on theoretical results obtained for **II**−H_2.

The Zn−H_{Zn} and O−H_O BLs (1.564 and 0.976 Å, respectively) lie in the range of values reported in the literature (the former ranges between 1.45[15a] and 1.71 Å,[13] the latter between 0.94[14] and 1.06 Å[12]) and quite close to those of Zn−H (1.60 Å) and O−H (0.97 Å) diatomic species.[44] Furthermore, the inspection of Figure 8 reveals that L_s^a keeps a quasitrigonal planar geometry, even if the H_{Zn} and the O(2) ions of the second layer are now involved in the coordination (L_s^a is 0.229 Å out of the plane of H_{Zn} and O(2) ions). As far as the coordination of L_s^b is concerned, it consists of a rather flat trigonal pyramid with L_s^b lying 0.431 Å out of the plane of Zn(2) ions and H_O. Incidentally, such an arrangement is quite similar to that of OD_3^+ cations in OD_3SbF_6.[60] The attainment and the maintenance of a 3-fold coordination by L_s^b is, again, not particularly surprising because it is very common for oxygen, where 4-fold coordination is limited to very few examples.[38]

Table 8. Theoretical Results for H_2 Chemisorbed on the ZnO(10$\bar{1}$0) Surface

	I−H_2	**II**−H_2	exptl
L_s^a−L_s^b (Å)	3.116	2.161	
L_s^a−H (Å)	1.561	1.564	
L_s^b−H (Å)	0.984	0.976	
H···H (Å)	1.989	2.403	
x_1 (Å)	0.092	0.431	
x_2 (Å)	3.208	2.574	
z_1 (Å)	1.116	1.116	
x_2 (Å)	1.078	0.836	
$\nu_{Zn-H_{Zn}}$ (cm^{-1})	1704 (1215)	1780 (1267)	1708 (1233)[b]
ν_{O-H_O} (cm^{-1})	3501 (2551)	3661 (2657)	3495 (2585)[b]
ν (cm^{-1})	1325 (1110)		
δ (cm^{-1})	828 (599)	770 (560)	840[b]
δ' (cm^{-1})	694 (501)	717 (521)	817[b]
BE (kcal/mol)	19	23	13[c]

[a] In parentheses are reported vibrational frequencies computed for the heterolytic dissociation of D_2 (type I). [b] From ref 9. [c] From ref 51.

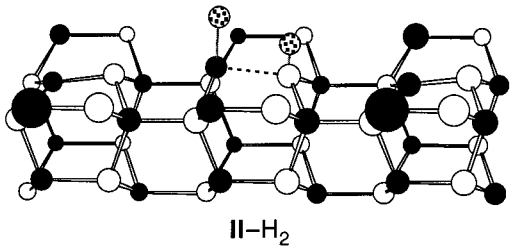

Figure 8. Schematic representation of the optimized geometry of **II**−H_2. Pseudoatom saturators are not reported in the figure for the sake of clarity.

(59) Maccato, C. Tesi di Dottorato University of Padova, 1998.

(60) Christe, K. O.; Charpin, P.; Soulie, E.; Bougon, R.; Fawcett, J.; Russel, D. R. *Inorg. Chem.* **1984**, *23*, 3756.

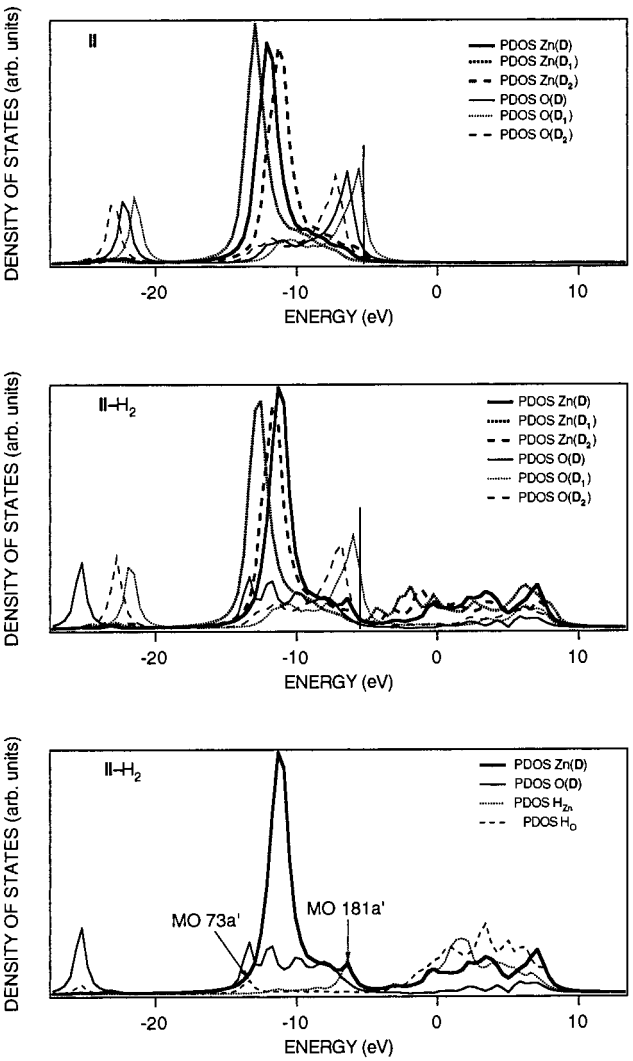

Figure 9. Comparison of the L_s^a and L_s^b PDOS of **D**, $\mathbf{D_1}$, and $\mathbf{D_2}$ in **II** and **II**$-H_2$; HL_s^a and HL_s^b PDOS are also reported. Vertical bars represent the energy of the HOMOs.

The L_s^a, L_s^b, H_{Zn}, and H_O Q values are 0.60, -0.66, -0.21, and 0.26, respectively, while the $L_s^a-H_{Zn}$ and $L_s^b-H_O$ OPs are 0.391*e* (the a′ component is 0.387*e*) and 0.286*e* (the a′ component is 0.266*e*),[61] respectively. It is interesting to note that $Q(H_{Zn})$ and $Q(H_O)$ are quite similar, contrary to data reported by Nyberg et al. (0.67 and 0.33, respectively).[14] Moreover, the $Q(L_s^a)$ decrease upon chemisorption (from 0.81 to 0.60) is almost completely compensated by the $Q(L_s^b)$ increase (from -0.83 to -0.66). These data, coupled to the significant $L_s^a-H_{Zn}$ and $L_s^b-H_O$ OPs, indicate that both L_s^a and L_s^b are significantly involved in the heterolytic dissociation of H_2 (see Figure 9). In Figure 10, the contour plots of the MOs mainly involved in the hydroxyl and hydride surface species are reported. Interestingly, the one mainly localized on $L_s^b-H_O$ accounts for a multicentered, totally bonding interaction extending over the whole $H_O-\mathbf{D}-H_{Zn}$ fragment. At variance to that, the one accounting for the $L_s^a-H_{Zn}$ bonding is $L_s^b-L_s^a$ antibonding. In good agreement with measurements carried out by Bolis et al.[51] for hydrogen reversibly adsorbed on ZnO (kadox), type I chemisorption is found to be exothermic by 23 kcal/mol (the experimental value is 13 kcal/mol).

(61) The $H_{Zn}\rightarrow L_s^a$ donation involves both the 4s (∼62%) and the $4p_z$ (∼35%) L_s^a AOs. Contemporary, the $L_s^a-L_s^b$ OP of **D** passes from 0.245 *e* in **II** to 0.057 *e* in **II**$-H_2$.

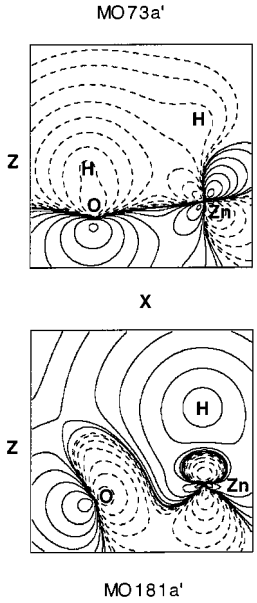

Figure 10. Two-dimensional contour plots of the **II**$-H_2$ 73a′ (above) and 181a′ (below) MOs in the *xz* plane. Contour values are $\pm 3.2 \times 10^{-3}$, $\pm 6.4 \times 10^{-3}$, $\pm 1.28 \times 10^{-2}$, ... $e^{1/2}$ Å$^{3/2}$ with negative values in dashed lines.

As in previous cases, vibrational analyses have been carried out on **I**. In Table 8, we have reported frequencies computed by using both the optimized parameters of **I**$-H_2$ and the ones computed for **D**, H_O, and H_{Zn} in **II**$-H_2$.[62] The very good agreement between experimental and theoretical ν computed with the *wrong* geometry is fortuitous. Actually, a careful analysis of the eigenvector relative to the ν at 1325 cm^{-1} indicates that it should be assigned to a $L_s^a-H_{Zn}$ bending mode,[63] which confirms the senselessness of the **I**$-H_2$ optimized geometrical parameters. In the latter case, the numerical agreement between experiment and theory is worse but still reasonable. Furthermore, vibrations at 770 and 717 cm^{-1} agree quite well with bands at 840 and 817 cm^{-1} assigned by Ghiotti et al.[9] and by Tsyganenko et al.[64] to bending modes of surface OH groups arising from the dissociative adsorption of H_2 on ZnO.[65]

4. Conclusions

Density functional calculations herein reported show that small saturated clusters are able to realistically model the L_s^a and L_s^b available on the clean and Cu-doped ZnO($10\bar{1}0$) surfaces and the molecular/dissociative adsorption processes occurring on them. The present data provide theoretical support to the Solomon proposal that exposed Cu(I) cations of CuCl(111) are good models of Cu(I) surface impurities of the Cu-doped ZnO-based catalyst. Calculations relative to the dissociative chemisorption of H_2 (type I) on ZnO confirm and reinforce our starting hypothesis that the dissociative chemisorption of Brønsted acids (B−H) to form strong L_s^a-B and L_s^b-H bonds significantly perturbs the surface geometry.

IC980443S

(62) The BE of H_2 on ZnO($10\bar{1}0$) by using **I** as a representative of the substrate and the optimized geometry of **II**$-H_2$ is 18 kcal/mol.

(63) Kokes et al.[2b] assumed for the δ_{Zn-H} frequency a value of 523 cm^{-1} by analogy with hydrides.

(64) Tsyganenko, A. A.; Lamotte, J.; Saussey, J.; Lavalley, J. C. *J. Chem. Soc., Faraday Trans. 1* **1989**, *85*, 2397.

(65) The eigenvectors relative to frequencies lying at 770 and 717 cm^{-1} indicate that the relative modes can be described as a frustrated translation out of the symmetry plane (the former) and in the symmetry plane (the latter).